KSME

Springer

Journal of Mechanical Science and Technology 34 (2) 2020

Original Article
DOI 10.1007/s12206-020-0104-9

Keywords:
· Spur gear
· Rolling bearing
· Time varying stiffness
· Backlash
· Dynamic analysis

Correspondence to:
Chan IL Park
pci@gwnu.ac.kr

Citation:
Park, C. I. (2020). Dynamic behavior of the spur gear system with time varying stiffness by gear positions in the backlash. Journal of Mechanical Science and Technology 34 (2) (2020) 565~572. http://doi.org/10.1007/s12206-020-0104-9

Received June 3rd, 2019
Revised August 20th, 2019
Accepted August 20th, 2019

† Recommended by Editor
No-cheol Park

Dynamic behavior of the spur gear system with time varying stiffness by gear positions in the backlash

Chan IL Park

Dept. of Precision Mechanical Eng., Gangneung-Wonju National University, Wonju 26403, Korea

Abstract Gear backlash is a nonlinear effect of the gear system. In a spur gear system with the backlash, the initial position of gears with the backlash affects the impact force. This work conducted a dynamic analysis of the spur gear system with time-varying mesh stiffness and bearing stiffness with a focus on the initial gear position within the backlash. For this purpose, the time-varying stiffness of the gears and rolling bearings were calculated. Mesh force with the time-varying stiffness and the gear backlash was applied to four DOF equations of motion. The equations of motion were solved using the Newmark beta method and Newton-Raphson method. The dynamic characteristics of the spur gear system by the initial position of gears within the backlash were investigated along with the magnitude of the backlash. The results showed that as the backlash increased, the mesh and bearing forces increased as well. The mesh and bearing forces were highly dependent on the initial gear position within the backlash. Significant initial mesh and bearing forces by the initial gear position within the backlash can lead to cumulative damages to the gear system.

1. Introduction

Spur gears have time-varying stiffness because of the gear meshing. Most spur gears are supported by the rolling bearings in the middle speed. The rolling bearings also have time-varying stiffness due to the changes in the loaded rolling elements. The time-varying stiffness of the gears and rolling bearings makes the spur gear system a parametric excited system. The rolling bearing stiffness has been reported by many studies described in a review paper [1]. While [2], Harris [3], Lim et al. [4-7], and Guo and Parker [8] proposed the bearing stiffness by the quasi-static bearing model. The vibration analysis of spur gears with the time-varying mesh stiffness was conducted by Umezawa et al., who experimentally validated the results [9]. Kim et al. conducted a dynamic analysis of the spur gears with the time-varying mesh stiffness and constant bearing stiffness [10].

The gear backlash and the time-varying stiffness of the spur gear system are the strong nonlinear factors affecting the spur gears. Gear backlash is given to the design phase to ensure good lubrication and the removal of the interference between teeth caused by manufacturing errors. The initial gear position within the backlash of gears is expected to have an effect on impact force. Regarding the backlash of spur gears, Kahraman and Singh investigated the nonlinear frequency response characteristics of spur gears with the backlash for external and internal excitations [11] and the nonlinear frequency response characteristics of the geared rotor-bearing system with the backlash and bearing radial clearances, which used the linear time-invariant mesh stiffness and simple bearing stiffness [12]. Lahmar and Velex analyzed the gear dynamic system with time-varying stiffness and bearing clearance, and found that bearings could produce the parametric excitations in helical gears [13]. He et al. applied the time varying mesh stiffness affected by gear eccentricity to the two stage spur gear dynamic model [14]. Park analyzed the tooth friction force and transmission error of spur gears due to sliding friction in quasi -static condition [15] and the spur gear system with time varying stiffness of

both gears and bearings [16]. However, in the spur gear system with time-varying stiffness of gear and rolling bearings, the dynamic characteristics by the initial gear position within the backlash of gears have not been reported.

This work conducts a dynamic analysis of the spur gear system with time-varying stiffness and backlash, which consists of gears, shaft, and rolling bearings. For this purpose, the time-varying mesh and rolling bearing stiffness are calculated and the four DOF equations of motion with mesh force are derived. Mesh force is classified in terms of the time-varying mesh stiffness, damping, and backlash according to the contact condition. Using the Newmark beta method and the Newton-Raphson method, the nonlinear behavior of the spur gear system is calculated. The dynamic mesh and bearing forces due to the time-varying mesh stiffness and dynamic behavior by initial positions of gears within the backlash are investigated as well.

2. The mathematical modeling

2.1 The stiffness of rolling bearings

In the quasi-static condition, the relation between the external load and the total load of the rolling elements with the bearing radial clearance of b_b at the angular position ψ_j is obtained. If the relation differentiated with the displacement δ_r, the stiffness of the rolling bearings can be given by [16, 17]

$$k_b = nk_n \sum_{j=1}^{H} (\delta_r \cos\psi_j - b_b)^{n-1} \cos^2 \psi_j \,. \tag{1}$$

where the values of n = 3/2 and n = 10/9 are used for ball bearings and roller bearings, respectively, and k_n is given by [2, 3]

$$k_n = \left[\frac{1}{(1/k_i)^{1/n} + (1/k_o)^{1/n}} \right]^n . \tag{2}$$

where k_i and k_o are the stiffnesses of the inner race and outer race for rolling elements, respectively [2, 3].

Assuming an initial radial displacement δ_r, the number of loaded rolling elements can be determined. Using the Newton-Raphson method, the total load of the loaded rolling elements is converged to the external force of bearings. The bearing stiffness can be obtained by substituting the converged radial displacement into Eq. (2).

2.2 Equations of motion

Driving and driven spur gears are modelled with the rigid cylinder of the base diameter and connected with the mesh stiffness as well as the damping along the line of action. Spur gears are supported with the stiffness and the damping of bearings, and the four DOF modelling is shown in Fig. 1.

Gear deformation is obtained by the translational displacement, the rotational displacement, and the static transmission error as follows:

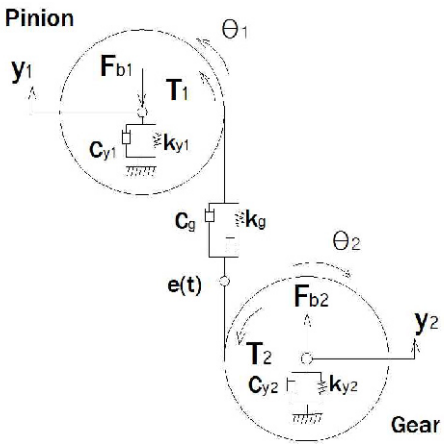

Fig. 1. Gear modeling.

$$\delta = y_1 - y_2 + r_{b1}\theta_1 - r_{b2}\theta_2 - e \,. \tag{3}$$

The static transmission error e is given by manufacturing errors, profile wear, and profile modification. If gears have the backlash, the mesh force is classified as the gear deformation-backlash conditions as follows:

$$F_g(t) = k(t)(\delta(t) - b) + c\frac{d\delta(t)}{dt} \quad \text{If } \delta(t) > b \,, \tag{4a}$$

$$F_g(t) = 0 \quad \text{If } |\delta(t)| \le b \,, \tag{4b}$$

$$F_g(t) = k(t)(\delta(t) + b) + c\frac{d\delta(t)}{dt} \quad \text{If } \delta(t) < -b \,. \tag{4c}$$

The bearing deflection can be approximated to be linear. Then, the linearized bearing force is given by

$$F_{yi}(t) = k_{yi}(t)y_i + c_{yi}\frac{dy_i}{dt} \,. \tag{5}$$

where k_{yi} is the combined stiffness of the bearing and the shaft. To examine the effect of bearing stiffness, the shaft is assumed to be rigid. In this case, the bearing stiffness becomes k_b.

Then, the four DOF equations of motion are derived by the mesh force, bearing force, input torque, and output torque applied to each gear as follows:

$$J_1\ddot{\theta}_1 = T_1 - F_g(t)r_{b1} \,. \tag{6}$$

$$J_2\ddot{\theta}_2 = -T_2 + F_g(t)r_{b2} \,. \tag{7}$$

$$m_1\ddot{y}_1 + F_g(t) + F_{y1}(t) = -F_{b1} \,. \tag{8}$$

$$m_2\ddot{y}_2 - F_g(t) + F_{y2}(t) = F_{b2} \,. \tag{9}$$

Table 1. Bearing data.

	Ball (SKF 6302)	Roller (SKF NU202)
No. of elements	7	11
Element diameter [mm]	7.938	5.5
Inner raceway diameter [mm]	23.7	19.3
Outer raceway diameter [mm]	33.7	27.9
Average raceway diameter [mm]	28.7	24.8
Roller width [mm]	-	19.3

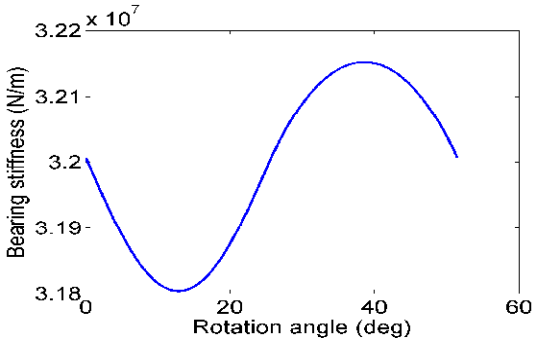

(a) Ball bearing stiffness

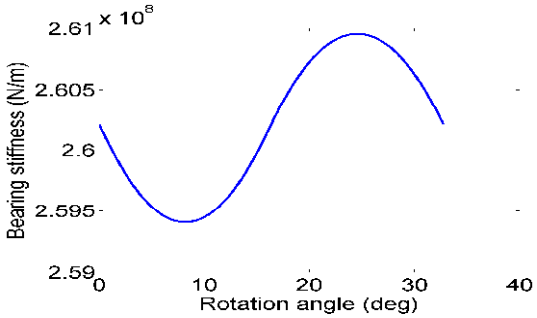

(b) Roller bearing stiffness

Fig. 2. Rolling bearing stiffness.

3. Analysis and discussion

3.1 The time-varying stiffness of rolling bearings and gears

To calculate the time-varying stiffness of the ball and cylindrical roller bearings without clearances, the ball bearing of SKF 6302 and the roller bearing of SKF NU202 with the bearing data shown in Table 1 are used.

Fig. 2 shows the ball and the roller bearing stiffnesses. The number of loaded rolling elements during rotation is changed, but the shape of the bearing stiffness is identical. The spur gears consist of three deformations: the bending and shear deformation, the gear foundation deformation, and the Hertz contact deformation. The force-deformation equation of the gears produces the gear mesh stiffness. The mesh stiffness on the input torque of 20 N·m is calculated using an in-house program, as shown in Fig. 3.

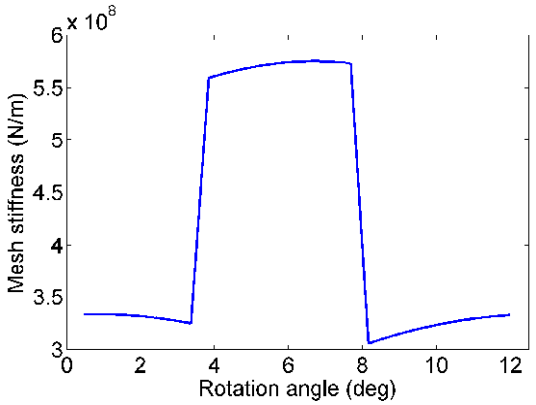

Fig. 3. Mesh stiffness.

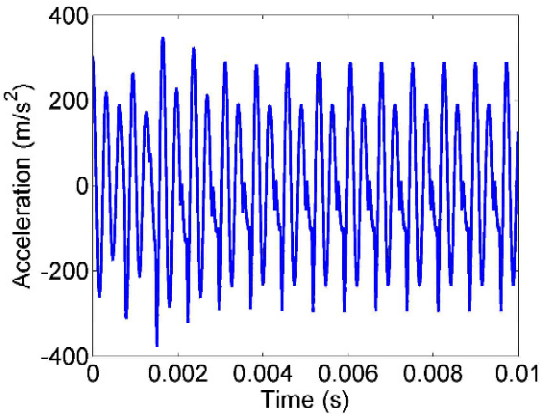

Fig. 4. Acceleration at the driving gear radius of 70 mm.

3.2 The dynamic analysis of the spur gear system

3.2.1 Validation of analysis model

To validate the analysis model, the time response of acceleration is compared with the results presented by Umezawa et al. [9]. The analysis of spur gears uses the same data as Ref. [9] along with the rotation speed of 1700 rpm. Since the model in Ref. [9] does not consider the stiffness of bearings and shafts, the relatively high stiffness of $k_{y1} = k_{y2} = 2 \times 10^{12}$ N/m is used for the present model. Using the Newmark beta method and the Newton-Raphson method, the acceleration at the driving gear radius of 70 mm can be calculated and plotted as shown in Fig. 4. The maximum acceleration by Umezawa's experiment was 227 m/s^2, and the analysis results are close to those of Umezawa's experiment, validating the current model.

3.2.2 Dynamic analysis by the gear position within the backlash

The gears are located in the middle of the shaft and supported by two bearings. Gear force is evenly divided into the bearing force. The dynamic analysis uses the spur gear data presented in Table 2. Using the spur gear data of Table 2, the effects of input torque, gear position in the backlash, and mag-

nitude of backlash are investigated. The gear and bearing damping coefficient are 0.07 and 0.01, respectively.

Dynamic analysis according to the gear position within the backlash is conducted. The input torque of 20 N·m and the backlash model of Fig. 5 with the half backlash of b = 30 μm are used. Initial position of a driving gear within the backlash is assumeds to be x = b, 0, -b of Fig. 5.

When the initial gear position is at x = 30 μm, x = 0 and x = -30 μm, the dynamic analysis results are shown in Figs. 6-8, respectively. Both the gear and the bearing exhibit the reduced steady-state force after the initial big transient force. The roller bearing produces a higher initial dynamic force than the ball bearing. As the gear position is located from x = 30 μm to x = -30 μm in the backlash, the maximum mesh force increases, except for x = 0 and x = -30 μm of gears with ball bearings, and generates more tooth separations. The maximum mesh force of gears with roller bearings is higher than that of gears with ball bearings. The maximum roller bearing force in the driving and driven shaft is larger than the maximum ball bearing force. However, the initial roller bearing force was greatly reduced while the ball bearing force was slowly reduced. The mesh and bearing forces are dependent on the initial gear position. In order to remove the initial transient component of bearing force, a bearing force after 0.02 seconds is analyzed in the frequency domain [18]. The ball bearing force has the dominant peak at about 2.7 kHz and the roller bearing force has the dominant peak at about 5 kHz. The ball bearing force in about 2.7 kHz is larger than the roller bearing force in about 5 kHz. This means that, although the maximum roller bearing force in the transient condition is bigger than the maximum ball bearing force, the ball bearing force after transient condition is larger than the roller bearing force.

Table 2. Data of spur gears.

	Driving gear	Driven gear
Normal module	2.0	
Pressure angle [deg]	20	
Center distance [mm]	58	
Whole depth [mm]	4.46	
Number of teeth	30	26
Face width [mm]	13	13
Base diameter [mm]	56.38	48.86
Pitch diameter [mm]	60.0	52.0
Coef. of add. mod.	0.57	0.55

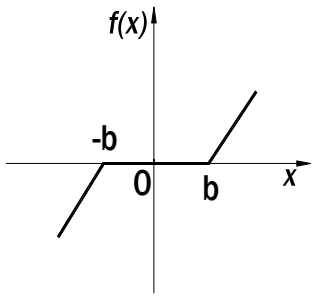

Fig. 5. Backlash model.

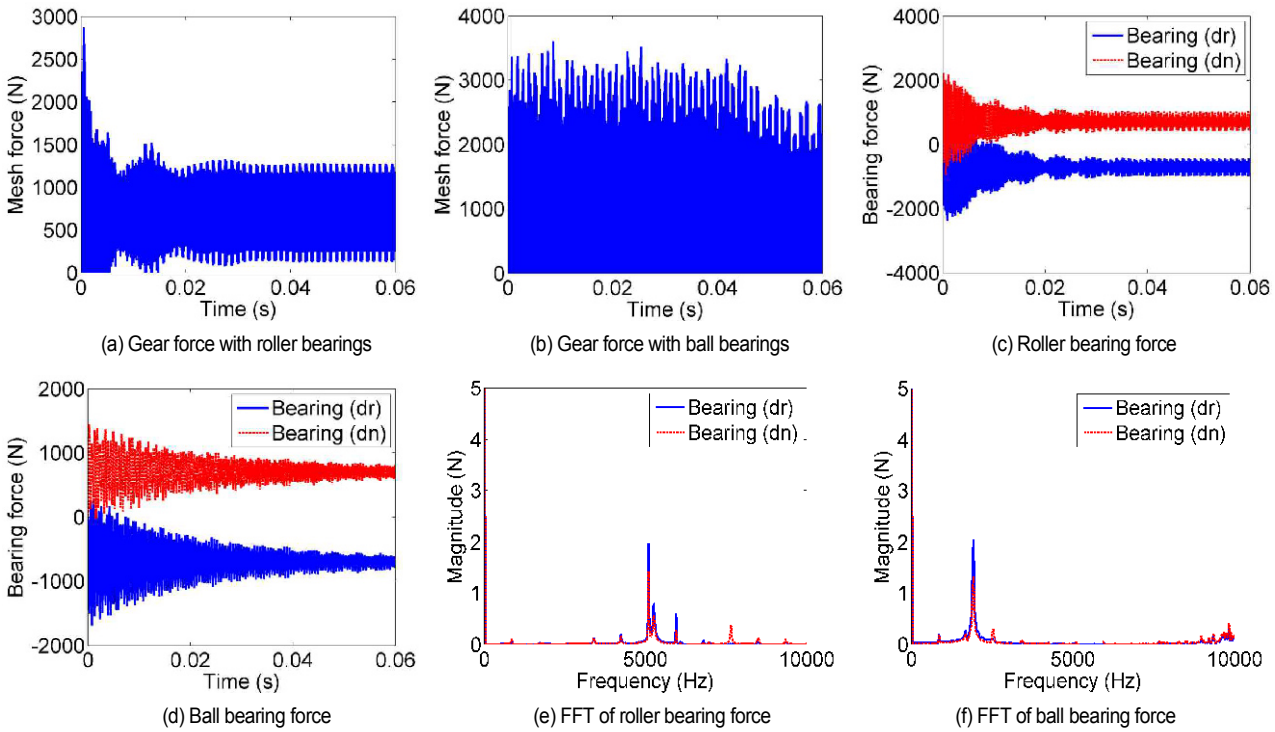

(a) Gear force with roller bearings (b) Gear force with ball bearings (c) Roller bearing force

(d) Ball bearing force (e) FFT of roller bearing force (f) FFT of ball bearing force

Fig. 6. Dynamic behavior of the gear system (x = 30 μm).

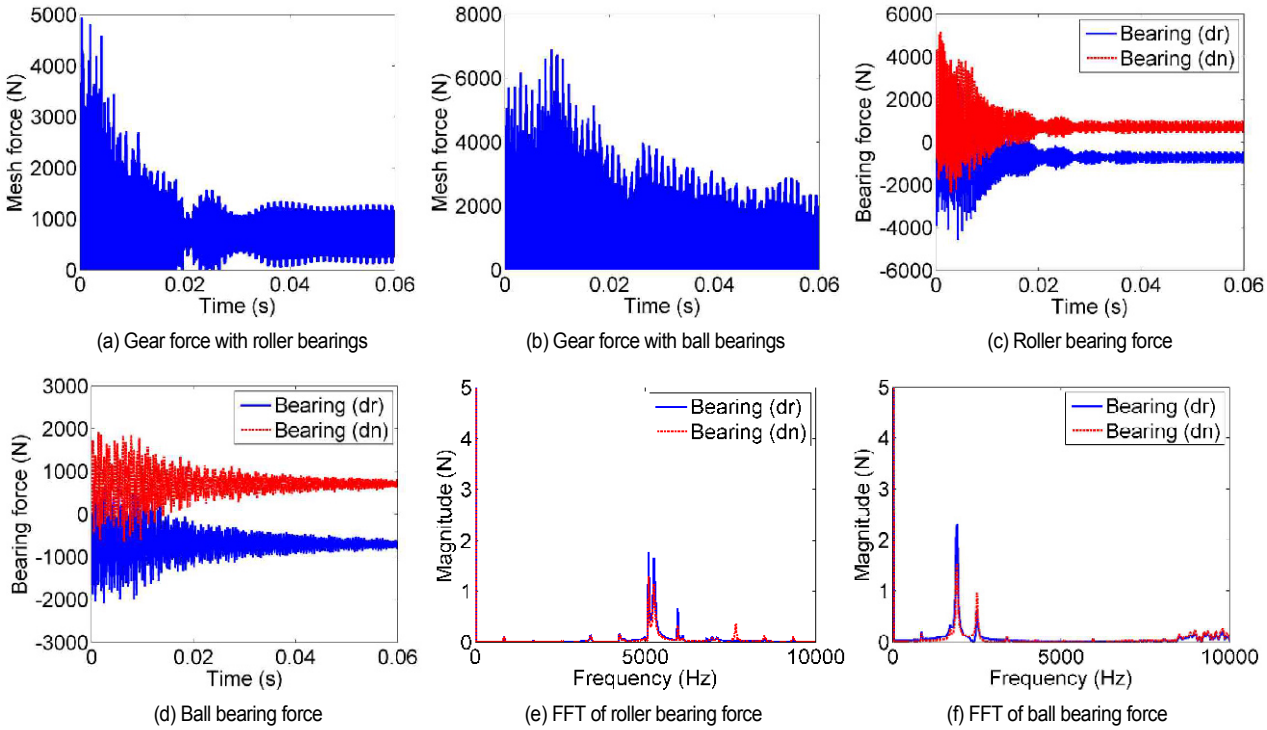

(a) Gear force with roller bearings (b) Gear force with ball bearings (c) Roller bearing force

(d) Ball bearing force (e) FFT of roller bearing force (f) FFT of ball bearing force

Fig. 7. Dynamic behavior of the gear system (x = 0, b = 30 μm).

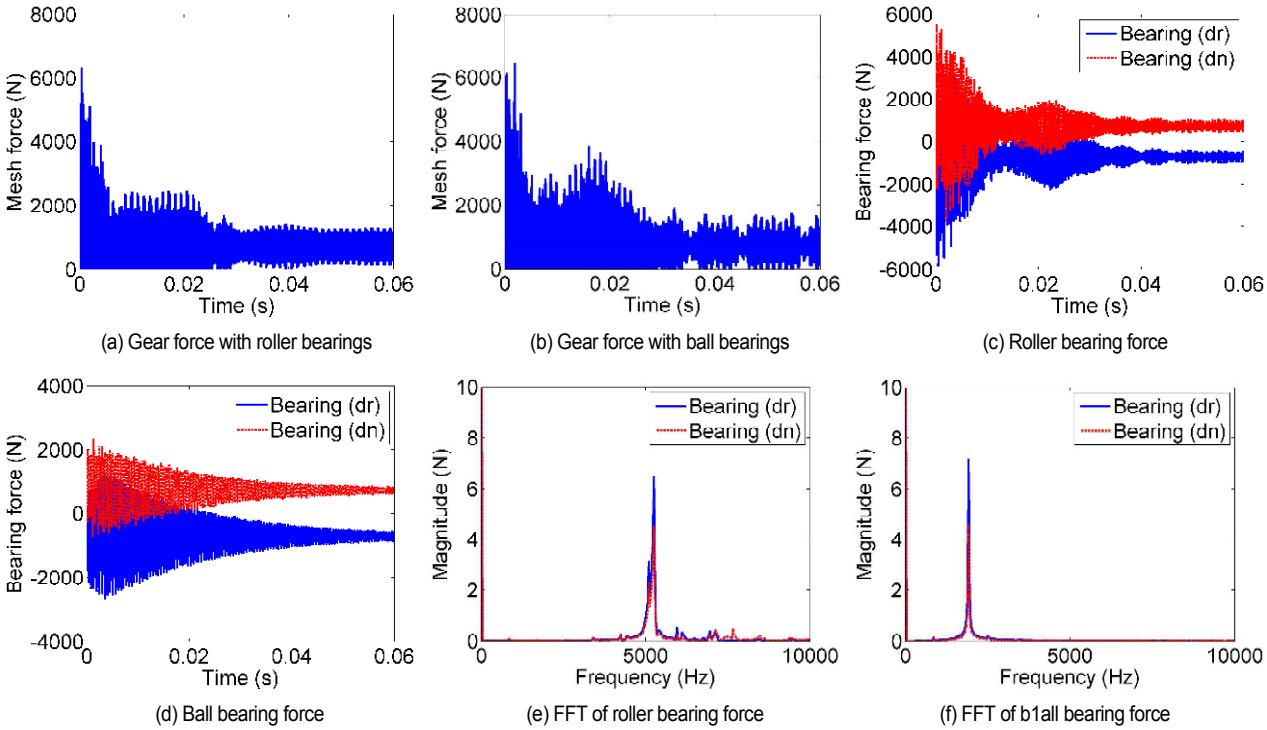

(a) Gear force with roller bearings (b) Gear force with ball bearings (c) Roller bearing force

(d) Ball bearing force (e) FFT of roller bearing force (f) FFT of b1all bearing force

Fig. 8. Dynamic behavior of the gear system (x = -30 μm).

3.2.3 Dynamic analysis by the backlash magnitude

As the half backlash increases from 30 μm to 100 μm, the maximum mesh and bearing forces significantly increase. Figs. 9-11 show the mesh and bearing forces as well as the FFT of bearing forces within the backlash of x = 100 μm, respectively. As the gear position is located from x = 100 μm to x = -100 μm within the backlash, the maximum mesh force increases, except for x = 100 μm of gears with ball bearings, and generates

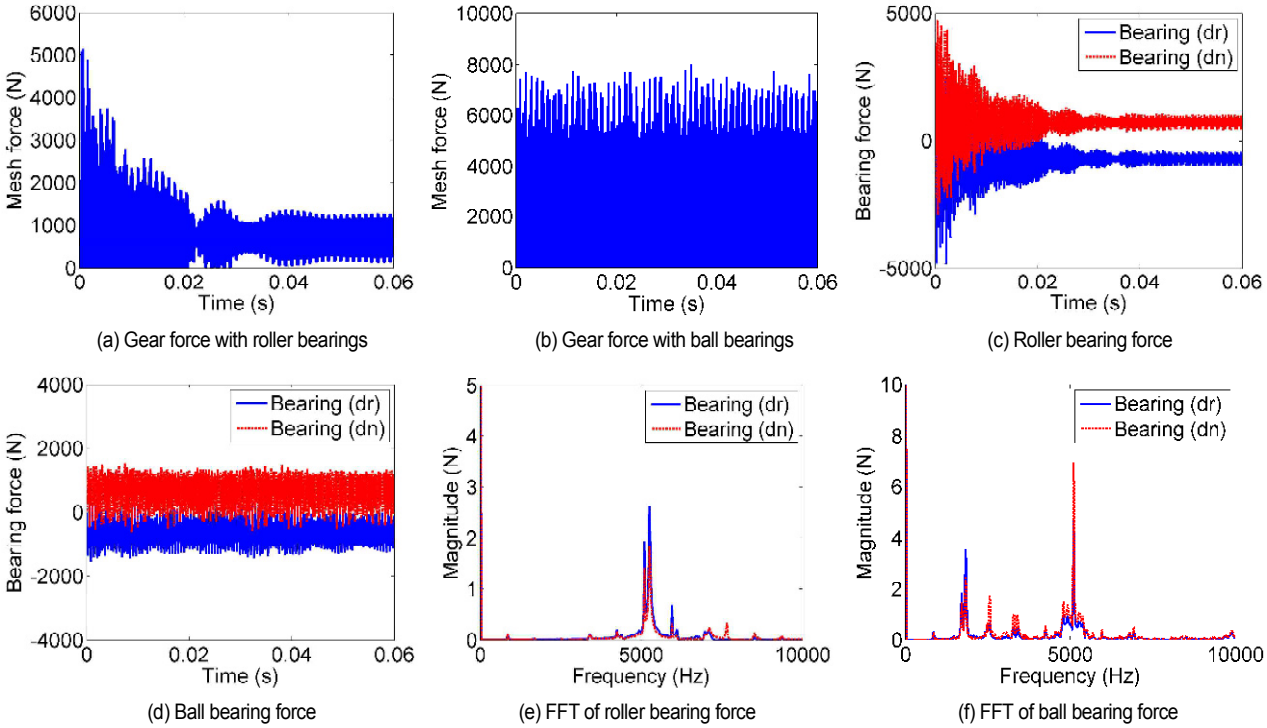

(a) Gear force with roller bearings (b) Gear force with ball bearings (c) Roller bearing force

(d) Ball bearing force (e) FFT of roller bearing force (f) FFT of ball bearing force

Fig. 9. Dynamic behavior of the gear system (x = 100 μm).

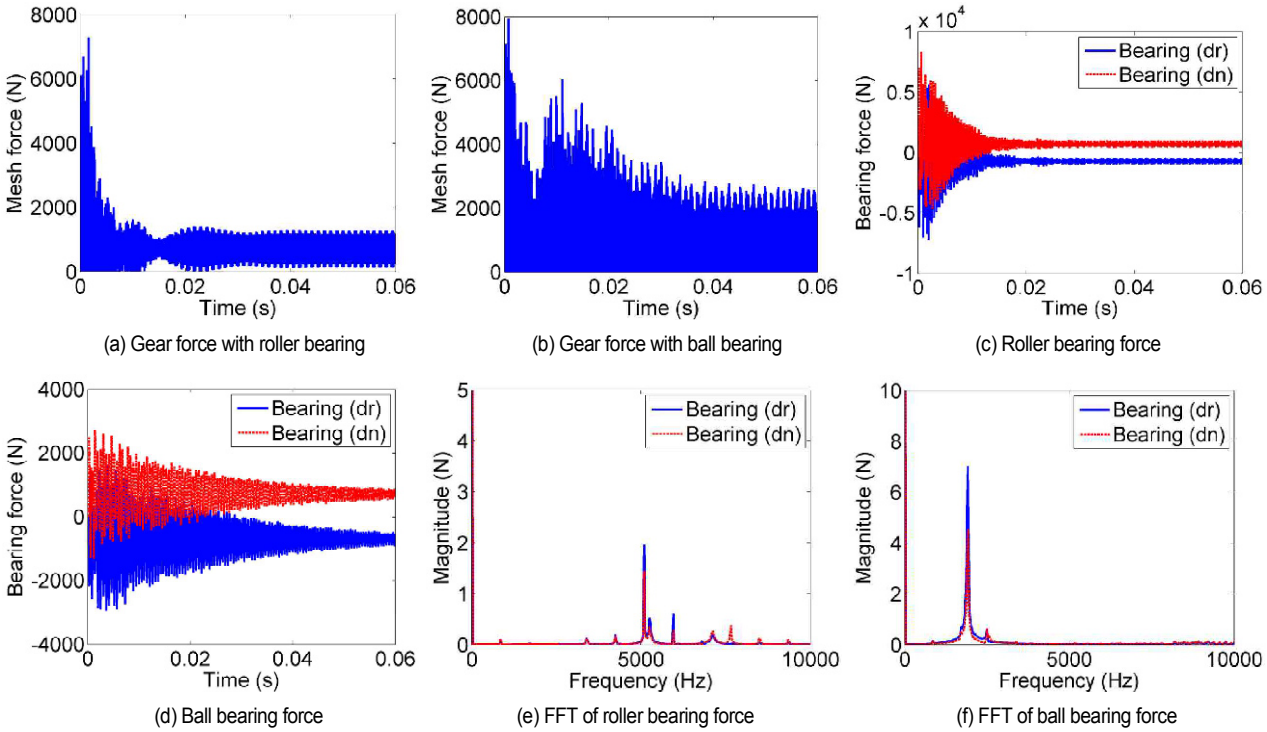

(a) Gear force with roller bearing (b) Gear force with ball bearing (c) Roller bearing force

(d) Ball bearing force (e) FFT of roller bearing force (f) FFT of ball bearing force

Fig. 10. Dynamic behavior of the gear system (x = 0, b = 100 μm).

more tooth separations. At x = 100 μm, the initial mesh and ball bearing force remain the same after the initial state.

The big initial mesh force causes rattle vibration in the gear system. As a result, the new peak around 5 kHz, except for 2.7 kHz, is produced in the FFT analysis. As the backlash increases, the initial mesh and bearing forces increase as well. In the FFT analysis of ball bearing force, the dominant peak around 2.7 kHz increases as the backlash increases. However,

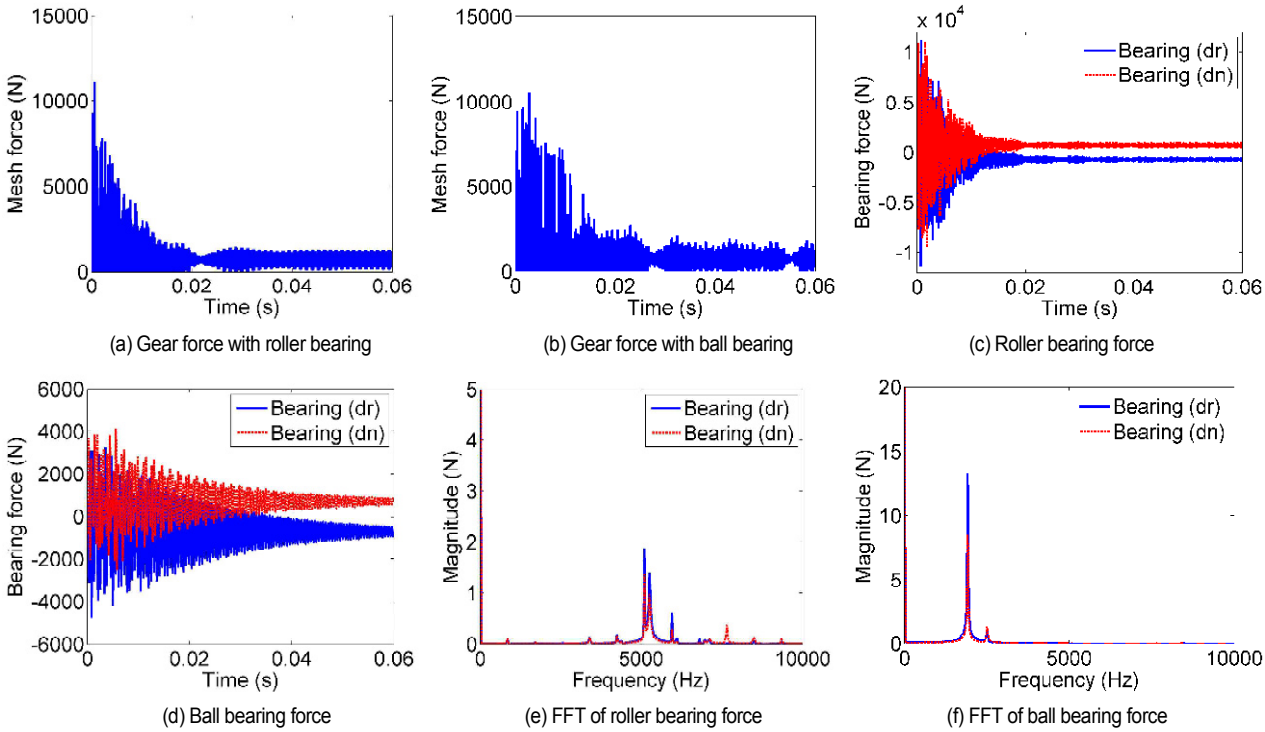

(a) Gear force with roller bearing (b) Gear force with ball bearing (c) Roller bearing force

(d) Ball bearing force (e) FFT of roller bearing force (f) FFT of ball bearing force

Fig. 11. Dynamic behavior of the gear system (x = -100 μm).

in the FFT analysis of roller bearing force, the magnitude of peaks around 5 kHz is almost the same, regardless of the gear positions.

Regarding the case of the half backlash of 30 μm, the mesh and bearing forces are highly dependent on the initial gear position within the backlash. As the initial gear position moves from x = 100 μm to x = -100 μm, the maximum mesh and bearing forces increase more than two times. Therefore, big initial mesh and bearing forces by the initial gear position within the backlash can lead to cumulative damages to the gear system, and help obtain information on the pre-failure of the gear system that cannot be obtained from the static analysis.

4. Conclusions

This work investigated the dynamic characteristics of the spur gear system with time-varying mesh stiffness and bearing stiffness by the initial position of gears within the backlash and the magnitude of the backlash. For this purpose, mesh force with the time-varying stiffness and the gear backlash were applied to four DOF equations of motion. As a result, the following conclusions were obtained:

(1) Both the gear and the bearing have the reduced steady-state force after the initial big transient force. The roller bearing produces a higher initial dynamic force than the ball bearing.

(2) As the initial gear position is located from x = 30 μm to x = -30 μm in the backlash, most of the maximum mesh and bearing forces increase and generate more tooth separations. The maximum roller bearing force in transient condition is bigger than the maximum ball bearing force, and the ball bearing force after transient condition is bigger than the roller bearing force.

(3) As the half backlash increases from 30 μm to 100 μm, the maximum mesh and bearing forces increase significantly. The mesh and bearing forces are highly dependent on the initial gear position within the backlash.

(4) Significant initial mesh and bearing forces by the initial gear position within the backlash can lead to cumulative damages to the gear system, and help obtain information on the pre-failure of the gear system that cannot be obtained from the static analysis.

Acknowledgments

This research was supported by Basic Science Research Program through the National Research Foundation of Korea (NRF) funded by the Ministry of Education (NRF-2017R1D1A3B03032458).

References

[1] S.-W. Hong and V.-C. Tong, Rolling-element bearing modeling: A review, *Int. J. Precision Eng. and Manuf.*, 17 (12) (2016) 1729-749.

[2] M. F. While, Rolling element bearing vibration transfer characteristics: Effect of stiffness, *Trans. ASME, J. Applied Mechanics*, 46 (Sept.) (1979) 677-684.

[3] T. A. Harris, *Rolling Bearing Analysis*, 4th Ed., John Wiley & Sons, New York (2001) 231-244.

[4] T. C. Lim and R. Singh, Vibration transmission through rolling element bearings, Part I: Bearing stiffness formulation, *J. Sound Vib*, 139 (2) (1990) 179-199.
[5] T. C. Lim and R. Singh, Vibration transmission through rolling element bearings. Part II: System studies, *J. Sound Vib*., 139 (2) (1990) 201-225.
[6] T. C. Lim and R. Singh, Vibration transmission through rolling element bearings. Part III: Geared rotor system studies, *J. Sound Vib*., 151 (1) (1991) 31-54.
[7] H. V. Liew and T. C. Lim, Analysis of time-varying rolling element bearing characteristics, *J. Sound Vib*., 283 (2005) 1163-1179.
[8] Y. Guo and R. G. Parker, Stiffness matrix calculation of rolling element bearings using a finite element/contact mechanics model, *Mech. Mach. Theory*, 51 (2012) 32-45.
[9] K. Umezawa, T. Sato and J. Ishikawa, Simulation on rotational vibration of spur gears, *Bulletin of JSME*, 27 (223) (1984) 102-109.
[10] W. Kim, H. H. Yoo and J. Chung, Dynamic analysis for a pair of spur gears with translational motion due to bearing deformation, *J. Sound Vib*., 329 (2010) 4409-4421.
[11] A. Kahraman and R. Singh, Non-linear dynamics of a spur gear pair, *J. Sound Vib*., 142 (1) (1990) 49-75.
[12] A. Kahraman and R. Singh, Non-linear dynamics of a geared rotor-bearing system with multiple clearances, *J. Sound Vib*., 144 (3) (1991) 469-506.
[13] F. Lahmar and P. Velex, Simulations of gear-rolling element bearing interactions in geared transmission, *Proc. of DETC '03*, DETC 2003/PTG-48040 (2003).
[14] X. He, X. Zhou, Z. Xue, Y. Hou, Q. Liu and R. Wang, Effects of gear eccentricity on time-varying mesh stiffness and dynamic behavior of a two-stage gear system, *Journal of Mechanical Science and Technology*, 33 (3) (2019) 1019-1032.
[15] C. I. Park, Tooth friction force and transmission error of spur gears due to sliding friction, *Journal of Mechanical Science and Technology*, 33 (3) (2019) 1311-1319.
[16] C. I. Park, Vibration analysis of the spur gear system with time varying stiffness of gears and bearings, *Proc. of the International Gear Conference 2018*, Lyon, France (2018) 806-814.
[17] C. I. Park, Stiffness effect of rolling bearings in the vibration analysis of the spur gear system, *Trans. Korean Soc. Mech. Eng. A*, 42 (5) (2018) 461-469.
[18] D. E. Newland, *An Introduction to Random Vibrations, Spectral & Wavelet Analysis*, 3rd Ed., Longman Scientific & Technical, Singapore, Ch 4, 10,12 (1993).

Chan IL Park, who received a B.S., an M.S., and a Ph.D. in mechanical engineering at Seoul National University, worked at Hyundai Motor Company for eight years. He was a dean of the College of Engineering at Kangnung National University for two years. He was the President of KSME and is a Professor in the precision mechanical engineering at Gangneung-wonju National University. His research interests are gears, plate, shell, optimal design, noise and vibration.